NANOSYSTEMS: PHYSICS, CHEMISTRY, MATHEMATICS, 2011, 2 (3), P. 29–36

UDC 538.958

COULOMB EFFECTS ON THE SPIN POLARIZATION OF QUANTUM RINGS

A. Manolescu[1], C. Daday[1,2], V. Gudmundsson[2]

[1]School of Science and Engineering, Reykjavik University, Reykjavik, Iceland

[2]Science Institute, University of Iceland, Reykjavik, Iceland

manoles@ru.is

PACS 71.70.Ej, 73.21.Hb,

We consider electrons in a circular nanoring of zero width, in magnetic field, and with Rashba spin-orbit interaction. We include the Coulomb interaction in the the "exact diagonalization" manner. The Coulomb interaction has strong effects on the spin polarization which may be totally different than for noninteracting electrons. Our current results include up to four electrons, but this number can easily be increased.

Keywords: quantum ring, spin-orbit interaction, Coulomb interaction.

1. Introduction

The spin-orbit interaction (SOI) of electrons in semiconductor nanostructures is in the center of the research in spintronics. This interaction mediates the influence of electric fields on the spin orientation of electrons, and thus the conversion of electric currents into spin polarization. Two well-known models of SOI are usually considered, one produced by the two-dimensional confinement of the electrons or Rashba [1] and another one due to the inversion asymmetry of the bulk crystal structure or Dresselhaus [2]. The strength of the Rashba SOI, α, may be modified with external electric fields created by external electrodes or gates, which is the main idea of the Datta-Das transistor [3], whereas the strength of the Dresselhaus SOI, β, is fixed by the crystal structure and by the thickness of the quasi two-dimensional electron system [4, 5]. In addition, in the presence of a magnetic field, an important effect on the electron spin is played by the Zeeman interaction which is determined by the effective $g-$factor, g^*, which depends on the material energy-band structure, being very small in GaAs but more that 100 times larger in InSb. Initial suggestions for spin-operated electronic devices were based on the Zeeman effect, but later this was deemed impractical because in general it is more desirable to achieve spin manipulation via an electric field than a magnetic field [6].

These three parameters, α, β, and g^*, determine together the spin polarization of electrons in quite a complicated way. Spin states and spin currents have been intensively studied on ring models [7–12]. Most works, however, do not include Coulomb interaction, or if they do, they are restricted to the simplest case of exactly two electrons like Refs. [11, 12]. Our model can treat a larger number of electrons, in principle limited only by the computational restrictions. In this paper we include up to four electrons.

If neither the Rashba nor the Dresselhaus coupling strength are negligible, then there will be a charge inhomogeneity on the ring. The density will have two maxima at angles $\frac{3\pi}{4}$ and $\frac{7\pi}{4}$ [10]. However, in our paper we consider only the Rashba SOI in combination with the Zeeman effect and the Coulomb repulsion. We use a discrete model of a 1D quantum ring. We describe the Coulomb effects completely using the method of exact diagonalization, also known as configuration interaction.

2. Ring model

We consider a one-dimensional circular quantum ring of radius R in a magnetic field B perpendicular to the plane of the ring described by the vector potential $\mathbf{A} = B/2(-y, x, 0)$. The general Hamiltonian of one electron with spin-orbit interaction is,

$$H = H_O + H_Z + H_{SO} \ , \tag{1}$$

where $H_O = \mathbf{p}^2/2m^*$ is the orbital Hamiltonian, with $\mathbf{p} = -i\hbar\nabla + e\mathbf{A}$ and m^* the effective mass of the electron in the semiconductor material, $H_Z = (1/2)g^*\mu_B B\sigma_z$ is the Zeeman Hamiltonian, g^* being the (material specific) effective g-factor. $H_{SO} = (\alpha/\hbar)(\sigma_x p_y - \sigma_y p_x)$ is the Rashba spin-orbit Hamiltonian, with α the SOI coupling parameter and $\sigma_{x,y,z}$ being the Pauli matrices.

We will use a discrete representation of the Hamiltonian, by defining N_φ sites around the ring. All sites have the same radial coordinate R. The angular coordinates are $\varphi_j = (j-1)\delta\varphi$, where $j = 1, 2, ..., N_\varphi$ and $\delta\varphi = 2\pi/N_\varphi$ is the angle between consecutive sites with the same radius. After a standard (symmetrized) discretization of the first and second angular and radial derivatives on this grid[1], we obtain the Hamiltonian in the position representation where the Hilbert space is spanned by the ket-vectors $|j\sigma\rangle$, where the integer j corresponds to the angular coordinate and $\sigma = \pm 1$ denotes the spin projection in the z direction. Such a discrete Hamiltonian has been often used in the recent literature [8, 9, 14].

In the basis $\{|j\sigma\rangle\}$ the matrix elements of the orbital Hamiltonian are obtained as follows:

$$\langle j\sigma|H_O|j'\sigma'\rangle = T\delta_{\sigma\sigma'}\left[\left(t_\varphi + \frac{1}{32}t_B^2\right)\delta_{jj'} - \left(t_\varphi + t_B\frac{i}{4\delta\varphi}\right)\delta_{jj'+1}\right] + h.c. \ . \tag{2}$$

We denoted $T = \hbar^2/(2m^*R^2)$ which we will use as energy unit. We will also consider R as length unit. We obtain the angular hopping energy, $t_\varphi = 1/\delta\varphi^2$ (in units of T), and $t_B = \hbar eB/(m^*T)$ the magnetic cyclotron energy. As usual $h.c.$ denotes the Hermitian conjugation of the previous terms.

The matrix elements of the Zeeman Hamiltonian are simply diagonal in the spatial coordinates,

$$\langle j\sigma|H_Z|j'\sigma'\rangle = \frac{1}{2}Tt_B\gamma\sigma\delta_{jj'} \ , \tag{3}$$

where $\gamma = g^*m^*/(2m_e)$ is the ratio between the Zeeman gap and the cyclotron energy, m_e being the free electron mass.

For the spin-orbit Hamiltonian we obtain:

$$\langle j\sigma|H_{SO}|j'\sigma'\rangle = \frac{1}{4}Tt_\alpha\left\{\frac{t_B}{2}\left[\sigma_r(\varphi_j)\right]_{\sigma\sigma'}\delta_{jj'} + it_\varphi^{1/2}\ \left[\sigma_r(\varphi_j) + \sigma_r(\varphi_{j+1})\right]_{\sigma\sigma'}\delta_{jj'+1}\right\} + h.\ c. \tag{4}$$

where $t_\alpha = \alpha/(RT)$ is the spin-orbit relative energy, while $\sigma_r(\varphi) = \sigma_x\cos\varphi + \sigma_y\sin\varphi$ and $\sigma_\varphi(\varphi) = -\sigma_x\sin\varphi + \sigma_y\cos\varphi$ are the radial and angular Pauli matrices, respectively.

The single particle states corresponding to the Hamiltonian (1), $H\psi_a = \epsilon_a\psi_a$, are calculated as eigenvalues and eigenvectors of the matrices (2)–(4). The eigenvectors are in fact spinors, meaning that the wave function of a quantum state a at any lattice site has the form

[1]The first and second derivatives of any generic function $f(x)$, are approximated as $f'(x) \approx [f(x+h) - f(x-h)]/2h$ and $f''(x) \approx [f(x+h) + f(x-h) - 2f(x)]/h^2$, respectively, where h is considered sufficiently small.

$\psi_a(\varphi_j) = \sum_\sigma \Psi_{a,\sigma}(j)|\sigma\rangle$, where $\Psi_{a,\sigma}(j)$ are $c-$numbers. Using now the single-particle states $\{\psi_a\}$ as a basis we write the many-body Hamiltonian in the second quantization as

$$\mathcal{H} = \sum_a \epsilon_a c_a^\dagger c_a + \frac{1}{2}\sum_{abcd} V_{abcd} c_a^\dagger c_b^\dagger c_d c_c \,, \tag{5}$$

where $c_a^\dagger$ and c_a are the creation and annihilation operators on the single-particle state a. The matrix elements of the Coulomb potential $V(\mathbf{r}-\mathbf{r}') = e^2/(\kappa|\mathbf{r}-\mathbf{r}'|)$, κ being the dielectric constant of the material, are in general given by

$$V_{abcd} = \langle \psi_a(\mathbf{r})\psi_\mathbf{b}(\mathbf{r}')|\mathbf{V}(\mathbf{r}-\mathbf{r}')|\psi_\mathbf{c}(\mathbf{r})\psi_\mathbf{d}(\mathbf{r}')\rangle \,. \tag{6}$$

In the present discrete model the double scalar product is in fact a double summation over all lattice sites and spin labels

$$V_{abcd} = Tt_C \sum_{j\sigma,\ j'\sigma'} \Psi^*_{a,\sigma}(j)\Psi^*_{b,\sigma'}(j')\frac{R}{|\mathbf{r}_j - \mathbf{r}_{j'}|}\Psi_{c,\sigma}(j)\Psi_{d,\sigma'}(j') \,. \tag{7}$$

The new energy parameter introduced by the Coulomb repulsion is $t_C = e^2/(\kappa RT)$. In the above summation over the sites the contact terms ($j = j'$) are avoided, their contribution vanishing in the continuous limit.

The many-body states are found by solving the eigenvalue problem for the Hamiltonian (5), $\mathcal{H}\Phi_\mu = E_\mu\Phi_\mu$. We do that by using the Hamiltonian matrix in the noninteracting many-body basis (Slater determinants), $\{|\alpha\rangle = |i_1^\alpha, i_2^\alpha, ..., i_K^\alpha\rangle\}$, where $i_a^\alpha = 0, 1$ is the occupation number of the single-particle state ψ_a and K is the number of single-particle states considered. The occupation numbers are listed in the increasing energy order, so ϵ_K is the highest energy of the single-particle states included the many-body basis. For any $|\alpha\rangle$ we have $\sum_a i_a^\alpha = N$, which is the number of electrons in the ring. It is straightforward to derive the matrix elements $\mathcal{H}_{\alpha\alpha'}$ using the action of the creation and annihilation operators on the many-body basis. This procedure is known as "exact diagonalization" or "configuration interaction". It does not rely on any mean field description of the Coulomb effects (like Hartree, Hartree-Fock, etc.), and it can be made convergent with K for a sufficiently small number of electrons, and a sufficiently small ratio of Coulomb to confinement energies, t_C.

To be able to carry the numerical calculations in a reasonable time we consider a small ring of radius $R = 50$ nm containing $N \leq 4$ electrons. The discretization is done in 100 angular points (sites). Common semiconductor materials used in the experimental spintronics are: InAs with $m^* = 0.023m_e,\ g^* = -14.9,\ \kappa = 14.6$, and estimated (or possible) values for the Rashba SOI $\alpha \approx 20$ meVnm; InSb with $m^* = 0.014m_e, g^* = -51.6, \kappa = 17.9$, and $\alpha \approx 50$ meVnm [4, 5]. The relative energies which we defined are: for InAs $t_\alpha = 0.60,\ t_C = 2.9, \gamma = -0.17$; for InSb $t_\alpha = 0.92,\ t_C = 1.5, \gamma = -0.36$. In our calculations we have considered material parameters somewhere in between these to sets, $\gamma = -0.2$ and $t_C = 2$. Since in general the SOI coupling constant may be tunable we have considered it variable, such that $0 \leq t_\alpha \leq 2$,

3. Results

3.1. Single-particle states

The single-electron eigenstates of the one-dimensional ring are analytically known. The Hamiltonian commutes with the total angular momentum $J_z = L_z + S_z$ and in the continuous limit ($N_\varphi \to \infty$) the eigenvectors are (see for example [10])

$$|\psi_a\rangle = \frac{1}{\sqrt{2\pi}} e^{il\varphi} \begin{pmatrix} c_{l\sigma} \\ -\sigma c_{l,-\sigma} e^{i\varphi} \end{pmatrix} \,, \tag{8}$$

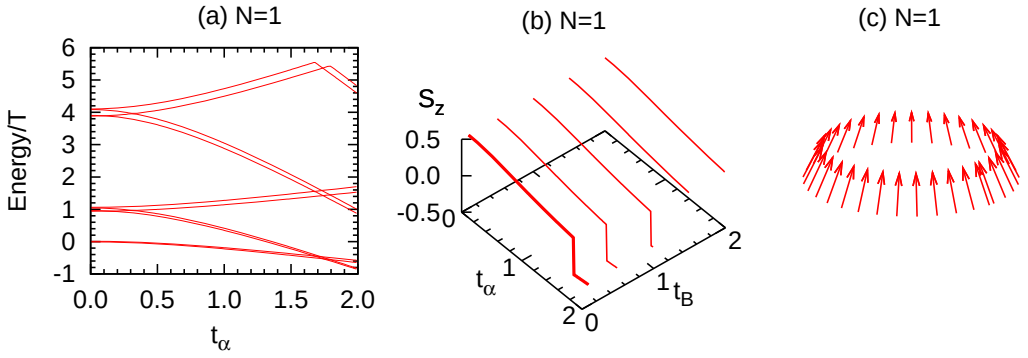

Fig. 1. (a) The lowest 10 energies of the single particle states vs. the SOI strength t_α. The magnetic energy is small, $t_B = 0.1$, such that the spin spitting is small. The spin spitting of the ground state is only barely visible. (b) The expected value of the spin projection along the z direction S_z, in units of $\hbar$, in the ground state, vs. t_α, for $t_B = 0.1, 0.5, 1.0, 1.5, 2.0$. The thicker line corresponds to the energy spectrum shown in (a). (c) The spin orientation around the ring in the ground state, for $t_\alpha = 0.5$ and $t_B = 0.1$ The angle with the z axis is about 27^o.

where $l = 0, \pm 1, \pm 2, ...$ is the orbital quantum number, and we have used the notations $c_{l,+1} = \cos(\theta_l/2)$, $c_{l,-1} = \sin(\theta_l/2)$. The angle θ_l is defined as

$$\theta_l = \tan^{-1}\left(t_\alpha \frac{4l + 2 + t_B}{4l + 2 + t_B - 2\gamma t_B}\right) , \tag{9}$$

which is the angle between the direction of the spin and the z axis. We see that for zero magnetic field ($t_B = 0$), or for zero g-factor ($\gamma = 0$), this angle is independent on the state. Obviously, in the absence of the SOI ($t_\alpha = 0$), $\theta_l = 0$ or π, i. e. the spin is parallel or antiparallel with the z axis. The energy spectrum corresponding to the eigenfunctions (8) is

$$\epsilon_a = \left(l + \frac{1}{2} + \frac{1}{4}t_B - \frac{\sigma}{2\cos\theta_l}\right)^2 - \frac{1}{4}(\tan\theta_l)^2 + \sigma\frac{\gamma t_B}{2\cos\theta_l} . \tag{10}$$

In Fig. 1 we show the energies of the single particle states obtained with the discrete model with 100 sites, in the interval of SOI strength $0 < t_\alpha < 2$ (units of T). The magnetic energy is $t_B = 0.1$ (units of T), which corresponds to a magnetic field strength of 0.013 Tesla. In this case the spin splitting is small, as seen in Fig. 1(a). The states are (doubly) spin-degenerate in zero magnetic field (Kramers degeneracy) for any $t_\alpha \neq 0$, but for $t_\alpha = 0$ only the ground state is doubly degenerate, the other states being degenerate four times. Not all intersections of the energy lines shown in Fig. 1(a) are real intersections. States with the same total angular momentum in reality repel each other and lead to avoiding crossings, but for the parameters used in this work this effect is not visible. (See for example Ref. [12].) Due to the SOI the energy of the states with S_z parallel to the effective magnetic field produced by the orbital motion decreases with increasing t_α, i. e. the states with $\sigma = +1$ and $l \geq 0$, or $\sigma = -1$ and $l < 0$. For the other states, with $\sigma = -1$ and $l \geq 0$, or $\sigma = +1$ and $l < 0$, the energy increases. In Fig. 1(b) we show the total spin in the ground state for several strengths of the SOI and magnetic field where a transition from spin-up to spin-down can be seen at strong SOI. The thicker line is calculated for the energies shown in Fig. 1(a), with $t_B = 0.1$ and a spin transition at $t_\alpha \approx 1.7$. The interval $0 < t_B < 2$ corresponds to $0 < B < 0.26$ Tesla. In Fig. 1(c) one can see the spin orientation in

the ground state for $t_B = 0.1$ and $t_\alpha = 0.5$. Since the magnetic field is small this angle is in this case close to $\tan^{-1} t_\alpha = 27^o$, according to Eq. (9). So we see that the results obtained with the discretized ring coincide with those corresponding to the continuous ring, given for example in Ref. [10].

3.2. Many-particle states

We will discuss now the results obtained for more electrons. In Fig. 2 we compare the energy spectra for the first 10 states vs. the magnetic energy for $N = 2, 3$, and 4 electrons, without and with Coulomb interaction. Since the Coulomb interaction is invariant at spatial rotations and independent on spin the total angular momentum is still a good quantum number. In other words the Coulomb term mixes many-body states with the same *total* J_z, and thus possibly with different spins. The spectra shown look different from the single-particle case, more or less like "spaghetti", but they are not very different with or without interaction. Most of the low-energy states decrease with increasing t_α because they are built on single-particle states with S_z along the effective magnetic field. There are two main effects of the interaction: One is the shift all energies to higher values, due to the net Coulomb charging. The other effect is that different states have different energy dispersion with t_α and so the level intersections or level repulsion may occur totally differently than in the absence of the Coulomb interaction. Consequently the spin states and the spin transitions may be totally different.

In Fig. 3 we show the total spin projected along the z direction, in the ground state, for several values of the magnetic energy. Because of the spin degeneracy, the results at zero magnetic field are not shown, but for the states shown they are very similar to those at $t_B = 0.01$, As before the thicker lines are calculated with the same magnetic energy used for the energy spectra, here $t_B = 0.5$. At this magnetic energy, the ground state for two electrons is close to a singlet type, or a spin compensated state, both with and without interaction, with $0 \leq S_z \leq 0.08$, as long as $t_\alpha < 1.55$, Fig. 3(a) and (b). Around this SOI strength, an intersection of the ground state with another state occurs in both cases. For the noninteracting case the new ground state is still of a singlet type, whereas for the interacting case it is mixed with a triplet state such that $S_z = 0.55$. At a lower magnetic energy, like $t_B = 0.01$, the ground state in the interacting case becomes again singlet at $t_B = 1.86$. At higher magnetic energies the ground state becomes triplet at zero or low SOI first in the interacting case (for example at $t_B = 1$), and then also for the noninteracting case (for example at $t_B = 1.5$).

More transitions can be seen for $N = 3$, for the interacting vs. the noninteracting case. For example at $t_B = 0.5$ in both cases the total spin is 0.5 at zero or low SOI strength, but at $t_\alpha \approx 0.3$ S_z becomes almost 1.5 with interaction, but almost -0.5 without interaction, as seen in Fig. 3(c) and (d). For $N = 4$ and $t_B = 0.5$ again a spin compensated state is preferred by the noninteracting system in the ground state for any SOI strength shown, whereas the interacting system has a configuration with $S_z \approx 1$ at zero and low SOI strength (three spins up and one down), as shown in Fig. 3(e) and (f). All these results are consequences of the mixing of different spin states with the same total angular momentum due to the Coulomb interaction. Examples with two electrons are also published in Refs. [11, 12].

Finally in Fig. 4 we compare the total spin for $N = 3$ and $N = 4$ electrons with and without Coulomb interaction, for equal SOI and magnetic energies, $t_\alpha = t_B = 0.5$. For $N = 3$, as described above, the projection of the total spin in the z direction is close to -0.5 (actually $S_z = -0.42$), but for the interacting state is close to 1.5 (actually $S_z = 1.39$). Obviously the quantized half-integer values are mentioned here only as reference values which have a meaning only in the absence of the SOI. In the next example, for $N = 4$ we compare an almost spin compensated state in the absence of the Coulomb interaction, $S_z = 0.01$, with a a spin polarized

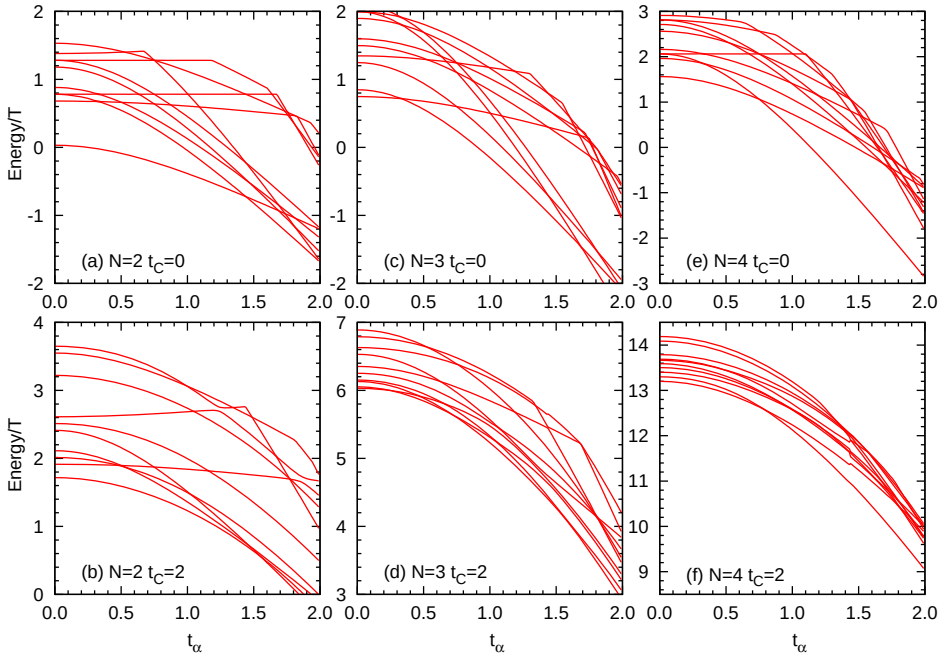

Fig. 2. Energy spectra of the lowest 10 states for $N = 2, 3$, and 4 electrons without Coulomb interaction, $t_C = 0$ in panels (a),(c),(e), and with Coulomb interaction, $t_C = 2$, in panels (b),(d),(f). The magnetic energy is $t_B = 0.5$. The variation of the energy with the SOI strength increases with the number of electrons and so the scale on the energy axes has been enlarged with N.

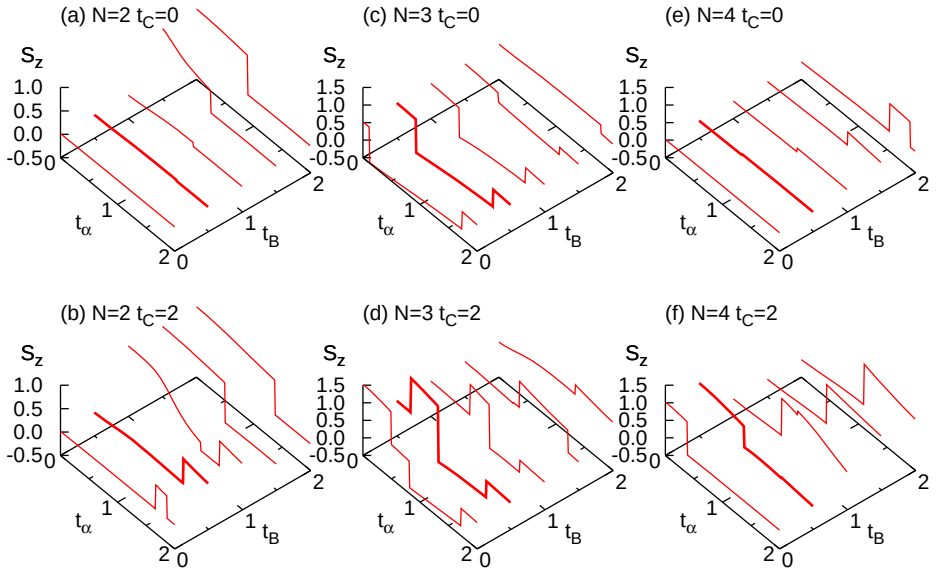

Fig. 3. Total spin of the many body states with $N = 2, 3, 4$ electrons, without interaction, i. e. $t_C = 0$ in panels (a),(c),(e), and with interaction, with $t_C = 2$, in panels (b),(d),(f), in the ground state, for magnetic energies $t_B = 0.01, 0.5, 1.0, 1.5, 2.0$. The thicker lines are for the same magnetic field as the energy spectra shown in Fig. 2.

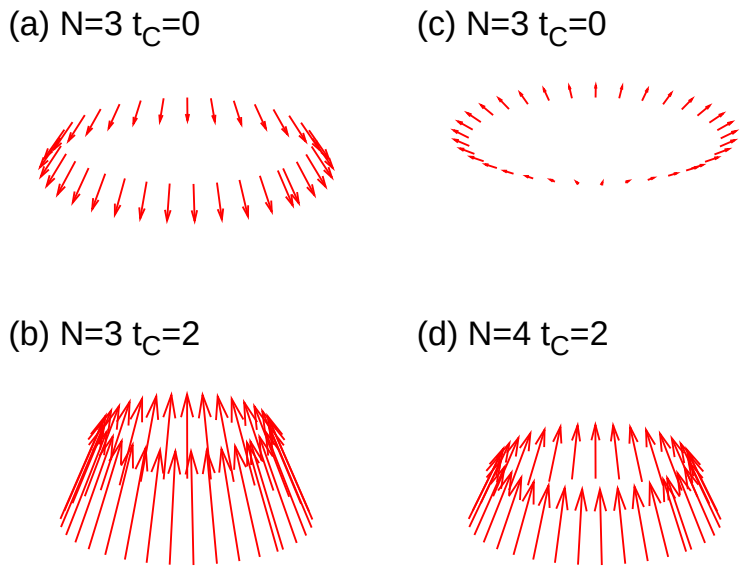

Fig. 4. The total spin orientation for $N = 3$ and $N = 4$ electrons, without Coulomb interaction, $t_C = 0$, and with Coulomb interaction, $t_C = 2$, in the ground state. The SOI energy is $t_\alpha = 0.5$ and magnetic energy is $t_B = 0.5$, like in Fig. 2.

state in the presence of the Coulomb interaction with $S_z = 0.91$. The excited states (not shown) may have totally different spin magnitude and orientations. In principle the direction of the total spin, which for $N = 1$ is given by the angle θ_l, is also determined by a mixing of states in the presence of the interaction. At low magnetic fields this angle is only slightly dependent on the state for the single particle states, but this variation may become much larger for the many-body states.

4. Conclusions

We calculated the many body states of a one-dimensional ring with $N \leq 4$, electrons with Rashba spin-orbit and with Coulomb interactions, in the presence of a magnetic field perpendicular to the surface of the ring. The Coulomb effects are fully included in the calculation via the "exact diagonalization" method. We used material parameters comparable to InAs and InSb materials. We observed strong (even dramatic) effects of the Coulomb interaction on the spin polarization both in the ground state and in the excited states which are illustrated with few selected examples.

Acknowledgments

This material was presented at the workshop Mathematical Challenges of Quantum Transport in Nano-Optoelectronic Systems, WIAS, Berlin, February 4-5, 2011 (OptoTrans2011). We wish to thank again to the organizers for this opportunity. We are also thankful to Catalina

Marinescu, Marian Niţă, and Sigurdur Erlingsson for valuable discussions. This research was supported by the Icelandic Research Fund.

References

[1] Bychkov Y. A., Rashba E. I. Oscillatory effects and the magnetic susceptibility of carriers in inversion layers // J. Phys. C: Solid State Phys. — 1984. — V. 17. — P. 60396045.
[2] Dresselhaus G. Spin-orbit coupling effects in zinc blende structures // Phys. Rev., II. Ser. — 1955. — V. 100. — P. 580–586.
[3] Datta S., Das B. Electronic analog of the electro-optic modulator // Appl. Phys. Lett. — 1990. — V. 56. — P. 665.
[4] Winkler R. Spin orbit coupling effects in two-dimensional electron and hole systems. — Berlin, Heidelberg, New York: Springer-Verlag, 2003.
[5] Ihn T. Semiconductor nanostructures. Quantum states and electronic transport. — Oxford University Press, 2010.
[6] Rashba E. I. Spin-orbit coupling and spin transport // arXiv cond-mat, Vol. 0507007v2:5, 2005.
[7] Molnar B., Peeters F. M., Vasilopoulos P. Spin-dependent (magneto)transport through a ring due to spin-orbit interaction // Phys. Rev. B. — 2004. — V. 69. — 155335.
[8] Splettstoesser J., Governale M., Zülicke U. Persistent current in ballistic mesoscopic rings with Rashba spin-orbit coupling // Phys. Rev. B. — 2003. — V. 68. — 165341.
[9] Souma S., Nikolići B. K. Modulating unpolarized current in quantum spintronics: Visibility of spin-interference effects in multichannel Aharonov-Casher mesoscopic rings // Phys. Rev. B. — 2004. — V. 70. — 195346.
[10] Sheng J. S., Chang K. Spin states and persistent currents in mesoscopic rings: Spin-orbit interactions // Phys. Rev. B. — 2006. — V. 74. — 235315.
[11] Liu Y., Cheng F., Li X. J., Peeters F. M., Chang K. Tuning of the two electron states in quantum rings through the spin-orbit interaction // Phys. Rev. B. — 2010. — V. 82. — 045312.
[12] Nowak M. P., Szafran B. Spin-orbit coupling effects in two-dimensional circular quantum rings: Elliptical deformation of confined electron density // Phys. Rev. B. — 2009. — V. 80. — 195319.
[13] Schliemann J., Carlos Egues J., Loss D. Nonballistic spin-field-effect transistor // Phys. Rev. Lett. — 2003. — V. 90. — 146801.
[14] Meijer F. E., Morpurgo A. F., Klapwijk T. M. One-dimensional ring in the presence of Rashba spin-orbit interaction: Derivation of the correct Hamiltonian // Phys. Rev. B. — 2002. — V. 66. — 033107.